THE ARCHIVE OF MECHANICAL ENGINEERING

Vol. L 2003 Number 3

Key words: *hydrodynamics, gasdynamics, oil consumption, piston engines*

*ANDRZEJ WOLFF**), *JANUSZ PIECHNA***)

NUMERICAL SIMULATION OF PISTON RING PACK OPERATION

The motion of a ring pack an oil film covering the cylinder liner has been considered. In the paper, equations, a numerical method, algorithm of solution and results of numerical simulations of this phenomena have been presented. The model presented takes into account hydrodynamic, spring and gas forces acting on each ring. The cases of motion with full and partial wetting of ring land have been considered. The influence of engine rotational speed, ring land curvature, oil viscosity on individual rings radial motion and oil film thickness have been analysed. The results of the calculations have been presented in graphical form.

1. Introduction

Piston rings, principally used to seal the gap between the piston and cylinder to prevent loss of combustion gases, are important components in internal combustion engines. Studies of piston ring performance have drawn attention of many researchers because of their importance in determining the mechanical efficiency, wear and fuel economy of an engine [1], [2], [8], [14].

To cover a wide range of duties like: sealing, lubrication and heat transfer, rings are constructed in packs. The typical pack consists of rings of different lip geometry, stiffness and thickness. In recent years, the number of rings in ring packs have been generally reduced from 5 to 3 rings [9].

This paper presents results of numerical simulation and parametric studies on a piston ring pack consisting of a barrel faced upper compression ring,

*) *Warsaw University of Technology, Faculty of Transport, ul. Koszykowa 75, 00-662 Warszawa, Poland; E-mail: wolff@it.pw.edu.pl*

**) *Warsaw University of Technology, Institute of Aeronautics and Applied Mechanics, ul. Nowowiejska 24, 00-665 Warsaw, Poland; E-mail: jpie@meil.pw.edu.pl*

a scraper second compression ring and a twin rail oil control ring used in a four-stroke engine. An integrated methodology has been applied which takes into account the complex interaction between the ring radial and axial motion, gas flow in the inter-ring regions, mixed lubrication at the ring-liner interface, oil transport, wear load and oil consumption.

The piston and ring pack are generally the greatest contributors to engine frictional losses. Engine manufacturers are continually looking for improvements in power output and efficiency, hence a reduction in piston and pack losses is sought [5], [13], [15].

The main objective of this investigation is to provide better predictions for ring minimum film thickness, friction, power loss, oil consumption due to scraping, inter-ring gas dynamics and ring motion. This is achieved by numerical investigation.

2. Technical problems

To prevent the leakage of the combustion gases through the necessary gap between the cylinder liner and piston, rings located in grooves in the piston wall are commonly used. To further reduce the friction between the cylinder liner and ring lips, a thin layer of oil between them is applied. Periodic motion of a piston with rings generates a variable oil film thickness between the cylinder liner and ring lips. This is associated with radial hydrodynamic forces tending to reduce the diameter of the ring. On the other hand, depending on the ring and groove geometry, combustion gases create radial gas dynamic forces acting to increase the ring diameter. Due to the variation of axial acceleration, rings can move axially inside the grooves, changing the contact between the ring's sides and groove.

Transferring these technical problems into the physical domain means that one has to recognise several physical phenomena required in a ring pack motion model [6], [7], [11].

3. Physical problems

Many physical phenomena are associated with ring pack operation, such as:

- ring dynamics for axial motion within the grooves to determine flow paths for gases,
- inter-ring gas dynamics for blow-by and blow-back behaviour,
- mixed lubrication at the ring face-liner conjunction for friction considerations,
- oil transport for distribution of lubricant along the liner,

- liner temperature influence on the oil viscosity and
- non-Newtonian phenomena associated with shear stresses typical for modern synthetic oils, had to be considered.

A flow of viscous fluid generally exists in a small gap between moving surfaces and a flow of gas through a small orifice between two volumes. Each ring has a small gap allowing a small variation of the ring diameter due to wear and cyclical changes of the oil film thickness. Each ring separates small volumes formed by the radial gap between the cylinder and piston and cylinder volume or crankshaft volume. These flows are coupled [12]. Pressure of the air or combustion gases, depending on the phase of the cycle, generates radial forces on the inner ring surfaces that tend to increase the ring diameter. Such a force in conjunction with the force due to elasticity of the ring must be in equilibrium with the hydrodynamic forces generated in the gap between the cylinder liner and ring lip. Gas forces depend on the thermodynamic processes inside the cylinder and the phase of the cycle. In contrast, the hydrodynamic forces depend on the oil film thickness, gap dimension and piston velocity. It can be assumed that generally gas forces are almost independent of the hydrodynamic forces. However, hydrodynamic forces strongly depend on the gas forces.

If the roughness of surfaces is taken into account, in some phase of the piston motion the gap between the cylinder liner and the ring lip is so small that it is necessary to consider the mixed lubrication problem.

Typically a great difference exists between the temperature of the upper and lower part of the cylinder liner. This means the temperature of the oil film also varies along the cylinder liner. Because the oil viscosity strongly depends on the oil temperature, liner temperature seems to be a key factor influencing the ring operation.

Modern oils have some non-Newtonian characteristics and typically viscosity depends on the local shear rate. As a result, such phenomena had also to be taken into account.

4. Mathematical model

The physical phenomena discussed above can be presented in the form of mathematical relations.

4.1. Flow of the viscous fluid in the gap between the cylinder liner and ring face

To describe this problem mathematically, it is necessary to make some assumptions:

1. An axi-symmetric approach is used for modelling the ring, with the ring back treated as gas dynamically loaded.
2. We assume that the ring-liner interface is filled with an incompressible fluid.
3. Viscosity of the fluid in the film is constant and is determined by the corresponding liner temperature and local shear rate.
4. The surface of the ring face can be partially or fully flooded.

With the above assumptions, flow in the gap can be described by the Reynolds equation.

In the case of ideal surfaces of the liner and ring the flow of the viscous fluid in the gap described by the Reynolds equation has the following mathematical form:

$$\frac{\partial}{\partial x}\left(\frac{\partial p}{\partial x}h^3\right) = 6\mu u\frac{\partial h}{\partial x} + 12\mu\frac{\partial h}{\partial t} \tag{1}$$

where

h – gap height,
p – pressure,
u – ring axial velocity,
t – time,
x – co-ordinate along the gap,
μ – dynamic viscosity.

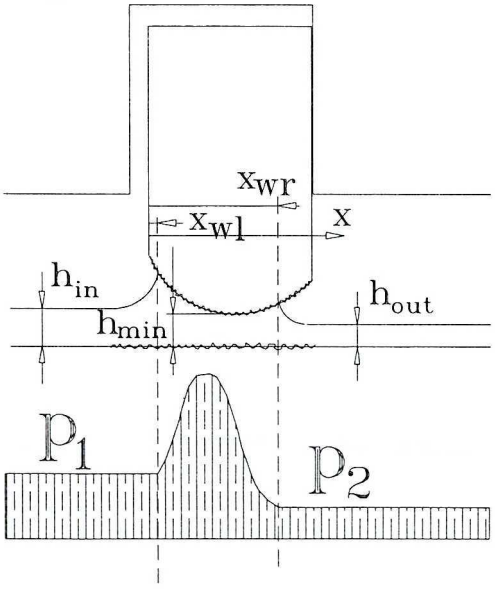

Fig.1. Parameters of the flow in the gap between the ring face and the cylinder liner in the case of partial lubrication

Conventional hydrodynamic analysis of sealing rings invariably predicts very thin oil films comparable to, or less than, typical surface roughness of the ring and liner. It is therefore essential to take account of asperity interaction and mixed friction. This will be the aim of the second part of this paper.

4.2. The geometry of the ring lip

The profile of the sealing ring is described by

$$h(x) = h_{\min} + \frac{(x - off)^2}{2R} \quad \text{for} \quad 0 < x < d \tag{2}$$

where $h_{\min}$ is the minimum gap height,
d is the ring width,
R is the ring surface radius,
off is the distance of $h_{\min}$ from the left ring edge, hitherto called offset in this paper.

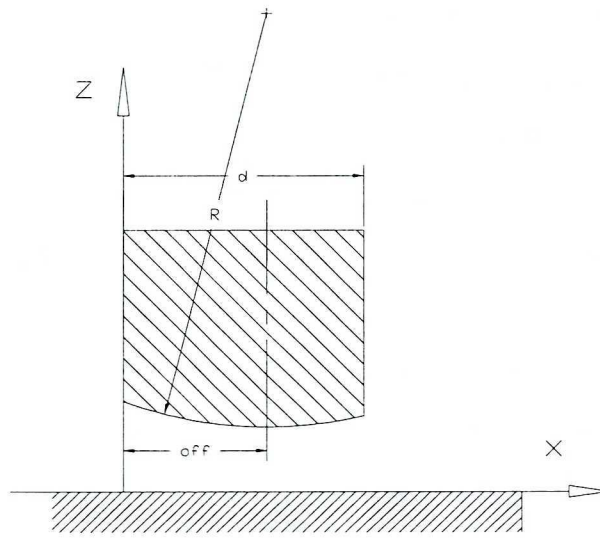

Fig. 2. Definition of the ring lip geometry

One problem is the definition of the profile geometry of the scraper ring. Initially manufactured as a linear oblique surface with sharp edges, after 600 hours of running it is worn out and its shape can be modelled as a parabolic with very large radius.

4.3. Boundary conditions

To preserve the solution of the Reynolds equation (1) it is necessary to describe the boundary conditions. Several different boundary condition formulations exist and after review it was decided that the following set of equations describes the physics of this phenomena in the best way.

The upstream boundary condition states that the hydrodynamic pressure is equal to the gas pressure (p_{gas_i}).

$$p(x_i) = p_{gas_i} \tag{3}$$

The downstream boundary condition states that the oil pressure is equal the gas pressure ($p_{gas_{i+1}}$) and the pressure gradient is equal to zero, which corresponds to the so-called "Reynolds assumption".

$$p(x_{i+1}) = p_{gas_{i+1}}; \quad \left.\frac{\partial p}{\partial x}\right|_{x_{i+1}} = 0 \tag{4}$$

We assume that the trailing edge of the ring is ventilated in the case of partial flooding.

The hydrodynamic force can be calculated by integration of the hydrodynamic pressure distribution as follows:

$$F_{hydr} = \int_{x_i}^{x_{i+1}} p(x)\,dx$$

4.4. Gas flows

From pressure variation measurements inside the cylinder during a full cycle of a single cylinder in operation, the pressure over the first sealing ring is known. In the presented work, variation of the pressure inside the cylinder is obtained by numerical simulation of the physical processes taking place inside the cylinder during the compression, expansion, exhaust and intake phases of a single cycle of operation. The pressure between the first, second and third rings can be calculated assuming an isentropic process of expansion and compression in the thin volumes between the rings. Taking into account the geometry and construction of the two-lip ring, it was assumed that no pressure difference exists across that type of ring. Due to the relatively high

pressure difference between these volumes, the gas dynamic equation including sonic and sub-sonic flows in orifices connecting volumes had to be used. It is assumed that gas leakage is limited only to the compensation gap between the ends of each ring.

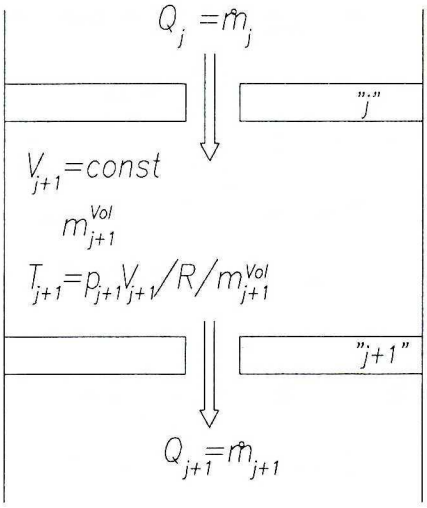

Fig. 3. Scheme of the gas flow though the ring compensation gap

In the case of subsonic flow through the ring compensation gap, the flow rate can be calculated by the following expression:

$$G = \alpha\beta A \frac{p_0}{\sqrt{T_0}} \sqrt{\frac{2k}{R(k-1)}} \sqrt{\left(\frac{p}{p_0}\right)^{\frac{2}{k}} - \left(\frac{p}{p_0}\right)^{\frac{k+1}{k}}} \tag{5}$$

where

p lower pressure,
p_0 higher pressure (stagnation pressure),
T_0 stagnation temperature in high pressure area,
k specific heat ratio,
R gas constant,
$\alpha\beta$ flow coefficients (contraction and velocity loss),
A area of the ring compensation gap.

In the case where the pressure ratio $\frac{p}{p_0} < \frac{p^*}{p_0}$, where $\frac{p^*}{p_0} = \left(\frac{2}{k+1}\right)^{\frac{k}{k-1}}$ applies, and defines the critical flow conditions, another form of equation is used. The critical flow rate is described as follows

$$G_* = \alpha\beta A \frac{p_0}{\sqrt{T_0}} \sqrt{\frac{k}{R}\left(\frac{2}{k+1}\right)^{\frac{k+1}{k-1}}} \tag{6}$$

Variation of the pressure inside the volume between rings filled by gas can be determined from the energy equation.

$$\frac{dp}{dt} = \frac{k-1}{V} \sum_{i=1}^{N} \alpha\beta\rho_i u_i A_i \left(\frac{kRT_i}{k-1} + \frac{u_i^2}{2}\right) \tag{7}$$

where

V gas volume between rings,

ρ density of the inflowing or outflowing gas,

u gas velocity.

The inner gas energy inside each volume is taken as a difference between the energy delivered from the volume of higher gas pressure and energy transferred to the volume of lower gas pressure.

4.5. Hydrodynamic, gasdynamic and spring forces

The local thickness of the gap between the liner and ring can be calculated from the force equilibrium conditions in the radial direction.

The hydrodynamic force acts in the radial direction on the ring, which must be compensated by the spring, gas pressure and friction forces in the cylinder groove. The inertia force in the radial direction has been neglected due to very small values of the radial ring velocity and the resulting small inertia forces.

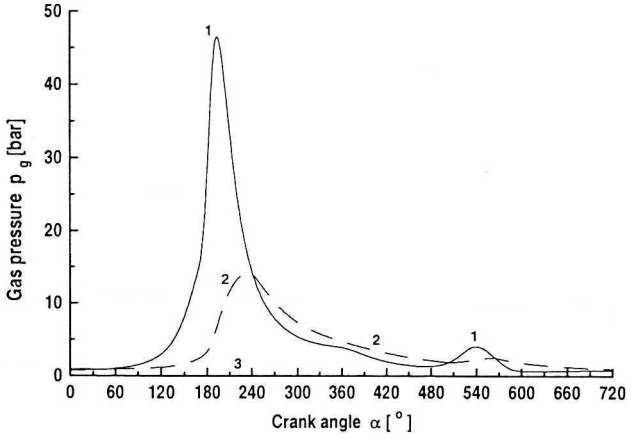

Fig. 4. Variation of the gas pressure acting on piston rings as a function of the crankshaft rotation (1 – compression ring, 2 – scraper ring, 3 – oil ring)

Fig. 4 presents the pressure variation between rings, calculated on the basis of the cylinder pressure variation due to gas leakage through the ring compensation gaps. One can notice the existence of phases of a relatively high pressure load on the upper (compression) ring. In some working phases, the radial gas force acting to increase the ring diameter is many times greater than the natural force from the ring stiffness in the same direction.

4.6. Friction force

The viscous friction force acting on the ring can be calculated by the following relationship:

$$F(t) = \int_{x_i}^{x_{i+1}} \left(\frac{h}{2} \frac{dp}{dx} - \mu \frac{u}{h} \right) dx \tag{8}$$

4.7. Power loss

The following relationship calculates the power loss including the power loss due to squeeze motion:

$$P(t) = u(t) F(t) + F_{hydr} \cdot v_{squeeze} \tag{9}$$

4.8. Oil motion

The ring lip surface area may be fully or partially wetted depending on the oil film thickness, axial ring velocity, gas pressure and ring stiffness. Expansion or contraction of the piston ring also has an influence on the wetted area of the ring land.

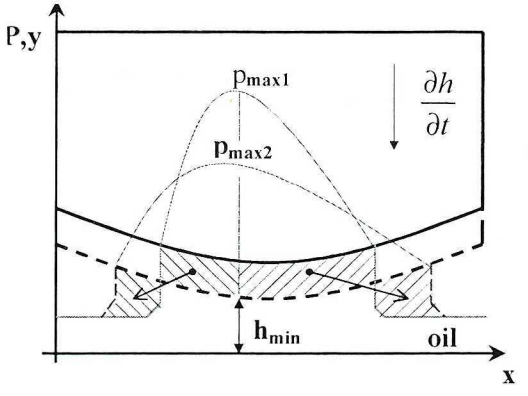

Fig. 5. Variation of the wetted area boundaries due to radial motion of the ring lip

The motion of each ring also transports the oil within the oil film. Some types of ring scrape and accumulate the oil in front of the ring. When the ring diameter is increased, some of the oil is pumped behind the ring. In the areas of starved oil flow, the thickness of the oil film becomes constant. In the presented model the oil flow is carefully calculated.

5. Numerical model

The numerical solution is based on the implicit finite difference scheme. The Reynolds equation (1) is discretized to form a set of linear equations which have a tri-diagonal matrix form, and can be effectively solved in each time step.

$$\frac{(h^n_{i-1/2})^3 p^n_{i-1} - \left((h^n_{i+1/2})^3 + (h^n_{i-1/2})^3\right) p^n_i + (h^n_{i+1/2})^3 p^n_{i+1}}{(\Delta x)^2} = 6\mu u^n \frac{h^n_{i+1/2} - h^n_{i-1/2}}{\Delta x} + 12\mu \frac{h^n_i - h^{n-1}_i}{\Delta t} \tag{10}$$

$$A p^n_{i-1} + B p^n_i + C p^n_{i+1} = D \tag{11}$$

where

$A = (h^n_{i-1/2})^3$,

$B = -\left[(h^n_{i-1/2})^3 + (h^n_{i+1/2})^3\right]$,

$C = (h^n_{i+1/2})^3$,

$D = 6\mu u^n \Delta x (h^n_{i+1/2} - h^n_{i-1/2}) + 12\mu(\Delta x)^2 \frac{h^n_i - h^{n-1}_i}{\Delta t}$.

A general solution of the ring motion problem was obtained in the following way. Assuming the gap between the liner and the ring lip is known, the vertical velocity (or squeeze velocity) is predicted, the pressure distribution is calculated, and the hydrodynamic force estimated and compared with the sum of the gas and ring stiffness forces.

$$v_{squeeze} = \frac{h^n_i - h^{n-1}_i}{\Delta t} \tag{12}$$

Depending on the difference between the force required and the force calculated, a correction of the vertical velocity is prescribed and a new calculation performed. These iterations are continued until the desired force equilibrium accuracy is reached.

$$F_{hydr}(v_{squeeze}) \approx F_{spring} + F_{gas} \tag{13}$$

6. Wetted area variation

In the case of starved lubrication, the main problem is to calculate the position of the left and right ends ($\mathbf{x}_{\text{left}}$ and $\mathbf{x}_{\text{right}}$) of the wetted part of the ring surface. Taking into account the position of maximum pressure and the velocity of the squeeze, the motion of the wetted area boundary is calculated from the continuity equation. The oil suppressed by the downward ring motion fills the areas in front and behind of the wetted zone.

In the case of fully flooded lubrication, it is assumed that a part of the oil film is accumulated in front of the ring lip or moved away by the ring.

It is also assumed that on one side of the ring system the cylinder surface is in the oil fog area. Due to adsorption the oil film thickness increases with the known velocity. On the opposite side of the ring pack, evaporation of the oil film is assumed.

It is also assumed that gas pressure existing on the left or right side of the ring acts on the back of the ring, depending on the direction of piston motion.

The oil cross flow rate through the ring is calculated as

$$q_{cross} = u\,\frac{h\left(x_{p_{\max}}\right)}{2} - v_{squeeze}\left(x_{right} - x_{left}\right) \tag{14}$$

where $h\left(x_{p_{\max}}\right)$ – a gap height at the point corresponding to the maximum pressure,

u – axial velocity of the ring,

$v_{squeeze}$ – squeeze velocity of the ring,

x_{left} – left boundary of the ring wetted area,

x_{right} – right boundary of the ring wetted area.

In the model used, some oil can be accumulated in the gap between the liner and ring lip during compression of the ring, and expelled during the ring decompression.

A modular approach is used to simulate the ring pack motion phenomenon. In this work, only some of these modules were used.

Generally, these modules resolve:
- ring axial dynamics within the grooves, which determine the flow paths for the gases,
- inter-ring gas dynamics for computing blow-by and blow-back,
- mixed lubrication phenomenon at the ring-liner interface, leading to estimated friction and power loss,
- liner oil transport (determination of lubricant availability for each ring and liner oil film distribution),
- oil consumption.

The general properties of this model and computer program have been verified by comparison with the results of code currently used by an engine manufacturer.

7. Oil consumption

The three main mechanisms of oil consumption are attributed to the ring pack system. These are:
- oil consumption due to evaporation,
- oil consumption from throw-off at the top ring due to inertia effects,
- oil entrained in the gases blowing into the combustion chamber.

The main problem is to determine the availability of oil for each consumption mechanism, and utilise this information to study the factors controlling it.

The model of oil consumption due to evaporation is based on the oil film thickness distribution on the liner and the ring pack motion corresponding to the phase when it is exposed to the high temperature combustion chamber gas. This happens during the down stroke of the piston, and the amount of oil is dependent on the lubrication conditions.

During the up-stroke, the scraping effect of the top ring is responsible for oil accumulation at the leading edge and partial redistribution on the liner. A fraction of this oil is discharged into the combustion chamber due to the inertia effects at the TDC reversal position.

During piston motion, some oil in the vicinity of the ring pack gets entrained into the flowing gas. This oil is taken from the oil film on the liner, oil at the end gap, oil at the leading and trailing edges of the rings and oil trapped between the asperities of the groove surfaces. The fraction of oil present in the gas-oil mixture flowing into the combustion chamber constitutes the consumption due to entrapment.

The model presented can resolve two types of ring lubrication phenomena. The ring surface can be fully or partially flooded, depending on the intermittent oil distribution. The leading edge of each ring face is either fully

flooded or the supply of oil for a particular ring is based on the oil film thickness formed by the trailing edge of the preceding ring resulting in a starved leading edge condition, implying lack of oil accumulation.

The model presented utilises the oil-fog scheme of oil film renovation. It assumes that under the piston an oil fog forms from very small uniformly distributed oil droplets. During the up-stroke, part of the liner oil film is rebuilt by adhesion of these oil droplets.

8. Results of calculation

The code incorporating the presented models has been used for simulating the commonly used ring set type consisting of a compression ring, a scraper ring and an oil ring. The geometry of the package is presented in Fig. 6. Two versions of the ring pack geometry used have been presented. The first package has all rings with symmetric lands, the second one uses asymmetric compression and scraper rings. Compression rings have number 1, scraper rings have number 2 and lips of the oil rings have numbers 3 and 4.

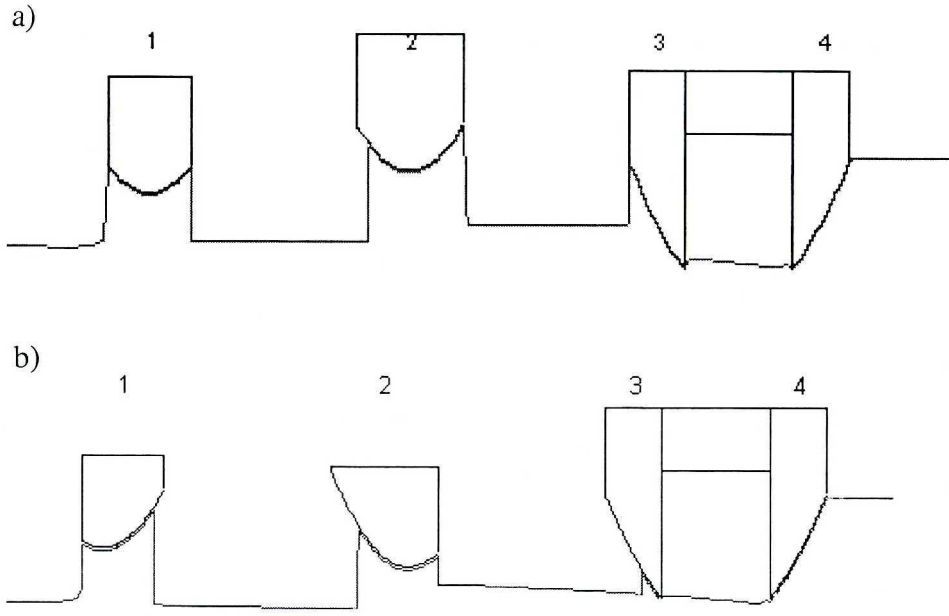

Fig. 6. Two considered ring pack geometry versions: a) symmetric ring profiles, b) asymmetric ring profiles (1 – compression ring, 2 – scraper ring, 3 – upper lip of the oil ring and 4 – lower lip of the oil ring), the continuous line represents the hypothetical oil film surface

In both cases, the two upper rings are single lip rings and the lower one is a two-lip ring. The shape of the ring land is controlled by two parameters: radius of curvature and offset. As a base, a symmetric type of land profile has been used. To improve the oil transportation capabilities, asymmetric ring land profiles were also considered.

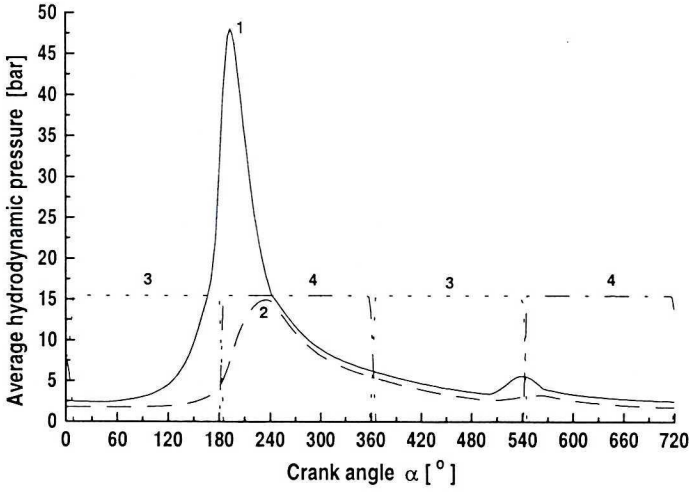

Fig. 7. Variation of the mean hydrodynamic pressure generated by each piston ring land as a function of the crankshaft rotation (1 – compression ring, 2 – scraper ring, 3 – upper lip of the oil ring and 4 – lower lip of the oil ring)

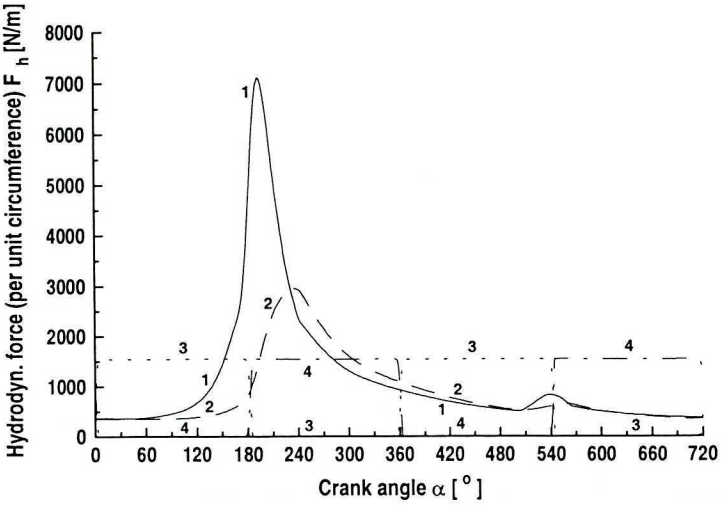

Fig. 8. Variation of the hydrodynamic forces generated by each piston ring land as a function of the crankshaft rotation (1 – compression ring, 2 – scraper ring, 3 – upper lip of the oil ring and 4 – lower lip of the oil ring)

Fig. 7 presents the mean hydrodynamic pressure and Fig. 8 the hydrodynamic force for each ring land necessary for compensating both the gas pressure and radial forces resulting from the ring stiffness. The oil ring has constant and rather strong spring load in comparison to the compression ring which exhibits low stiffness but is strongly influenced by the gas forces. Variation of the scraper ring load is similar to the compression ring load but the maximum load values are approximately halved.

Using equation (8), we calculated friction forces for each ring pack as functions of the crankshaft rotation.

The friction force contribution of each ring is presented in Fig. 9.

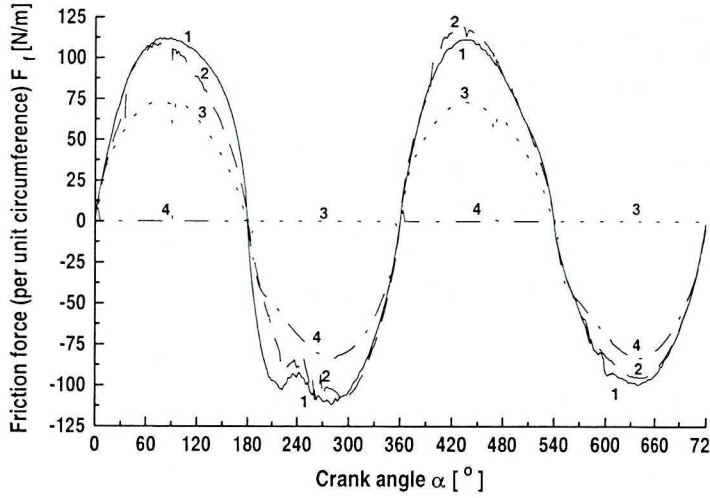

Fig. 9. Variation of the unit tangential forces acting on each piston ring as a function of the crankshaft rotation (1 – compression ring, 2 – scraper ring, 3 – upper lip of the oil ring and 4 – lower lip of the oil ring)

Total friction power losses can be calculated by the use of equation (9).

Fig 10 shows variation of the power losses as a function of the crankshaft rotation.

The oil film thickness can be calculated from the pressure distribution in the gap between the ring land and the liner. The results of such calculation are presented in Fig 11.

The top ring has lower minimum film thickness values during the expansion stroke due to a higher gas load (groove pressure) compared to other portions of the cycle. The second ring has lower minimum film thickness value on the down-strokes than the up-strokes due to its scraper face profile. In both cases, there is not much difference between the minimum film thickness values for the oil ring rails. This can be attributed to the fact that the

oil ring is quite insensitive to the low groove pressure acting behind it and it is the high installed tension force which causes significant scraping, thereby promoting substantial oil accumulation at the leading edges even with a relatively low oil supply. As a result, the minimum film thickness behaviour for the oil ring shows low sensitivity to oil supply conditions.

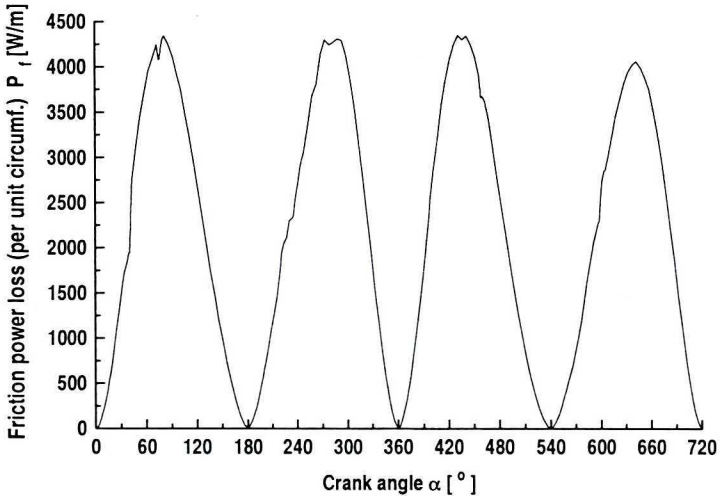

Fig. 10. Ring power losses as a function of crankshaft rotation

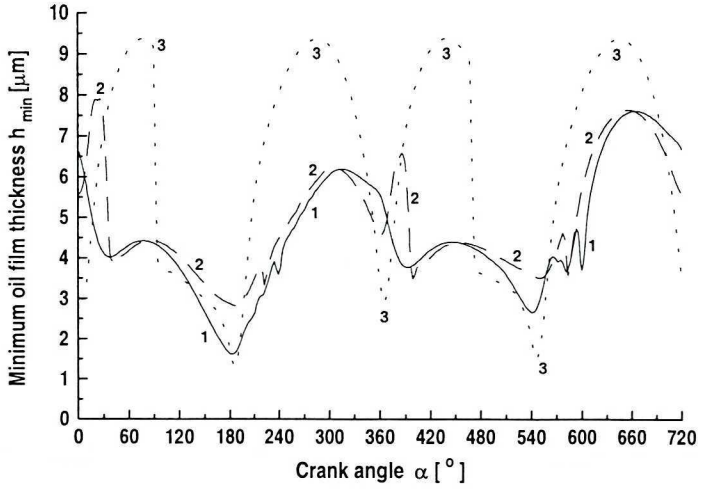

Fig. 11. Variation of the ring land-liner distance as a function of the crankshaft rotation (1 – compression ring, 2 – scraper ring, 3 – oil ring)

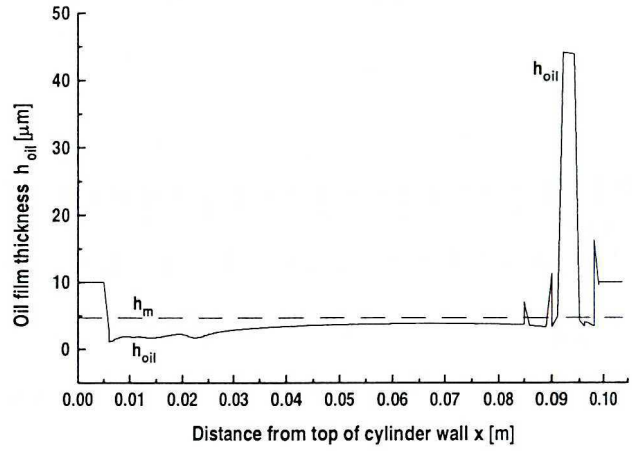

Fig. 12. Variation of the oil film thickness left by the ring pack

The motion of the ring pack scraping and distributing oil on the cylinder liner leaves the oil film profile shown in Fig. 12 after a few cycles of operation. Low oil film thickness near the top dead centre and peaks of accumulated oil near the leading ring lips can be clearly seen.

By changing the co-ordinate system from the global to the local system of the ring set, one can calculate the oil flow rate incoming to each ring, scraped oil accumulated in front of each ring and oil flow rate passing in the gap between the ring land and cylinder liner.

For each ring, the amount of oil belonging to these groups of flow parameters can be calculated.

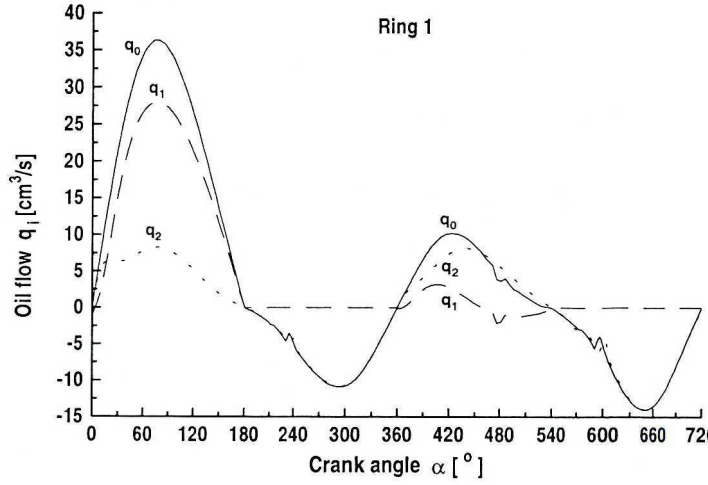

Fig. 13. Compression ring oil flow rate as a function of crankshaft rotation: q_0 oil flow rate entering the leading edge; q_1 flow rate of the scraped oil, q_2 oil flow rate leaving the trailing edge

In Fig. 13 the oil flow rates corresponding to the first (compression) ring are presented. One can clearly see the phases of the ring motion when the ring is only partially flooded and slides on the oil film. The oil is scraped during the motion towards the top dead centre (0–180 and 360–540 deg) and the ring slides during the motion away from top dead centre (180–360 and 540–720 deg). Negative scraped oil flow rate describes the negative direction of the piston motion during down-strokes.

A set of data similar to Fig. 13 is shown in Fig. 14, corresponding to the second (scraper) ring. One can notice a different mode of ring operation. This ring scrapes the oil mainly during the downstroke (180–360 and 540–720 deg).

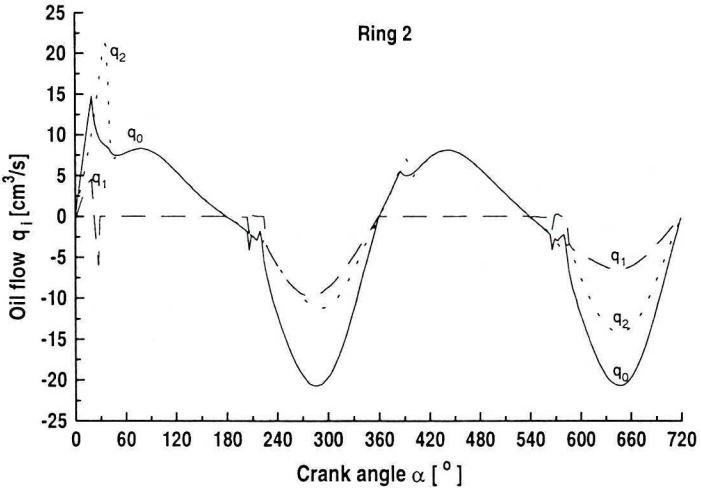

Fig. 14. Scraper ring oil flow rate as a function of crankshaft rotation: q0 oil flow rate entering the leading edge; q_1 – flow rate of the scraped oil, q_2 – oil flow rate leaving the trailing edge

Fig 15 includes data for the last two-land (oil) ring. Each of the ring lips works in a different way. The oil rings scrape the oil during the motion away from TDC. The lower ring lip is more efficient. Only near piston reversal points both ring lips work together.

Of greatest interest is the information about the amount of oil scraped by each ring, accumulated in front of it and redistributed along the liner. Fig 16 presents the data allowing comparisons between the scraping efficiency of the considered ring types. The most important are values near the turning points (180, 360, 540, 720). It can be seen that the compression ring delivers some oil to the combustion chamber (points 180 and 540). By contrast, the oil ring scrapes oil into the crankcase

(points 360 and 720). The scraper ring only scrapes and redistributes oil on the liner.

a)

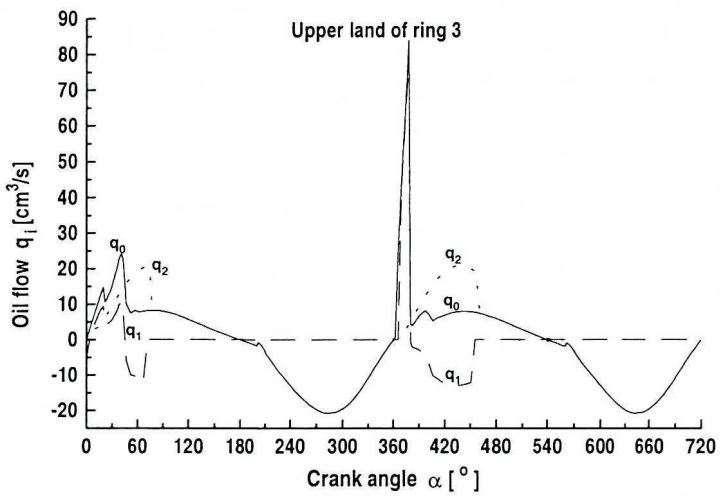

b)

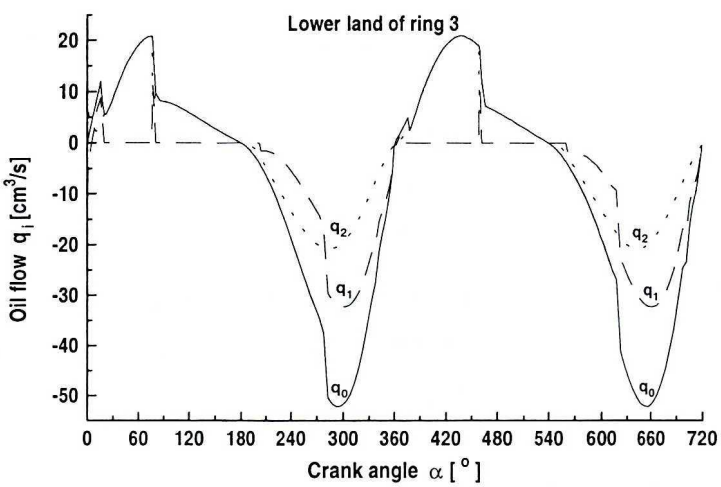

Fig. 15. Two-land oil ring oil flow rate as a function of crankshaft rotation: q_0 oil flow rate entering the leading edge, q_1 – flow rate of the scraped oil, q_2 – oil flow rate leaving the trailing edge. a – upper ring lip, b – lower ring lip

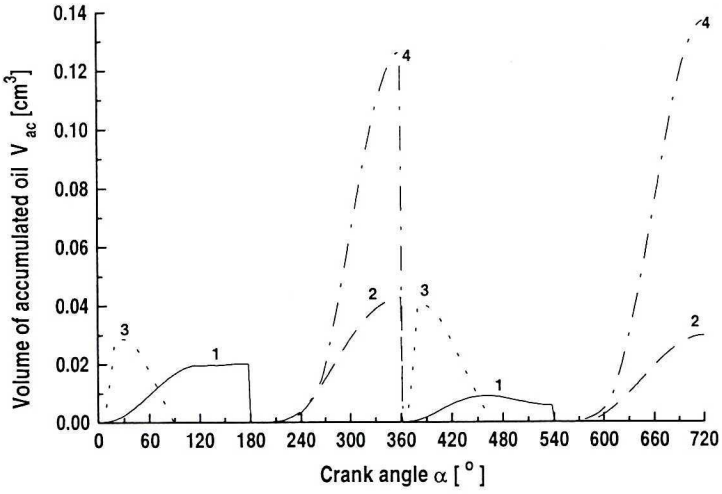

Fig. 16. Volume of oil accumulated by each ring as a function of crankshaft rotation (1 – compression ring, 2 – scraper ring, 3 – upper lip of the oil ring and 4 – lower lip of the oil ring)

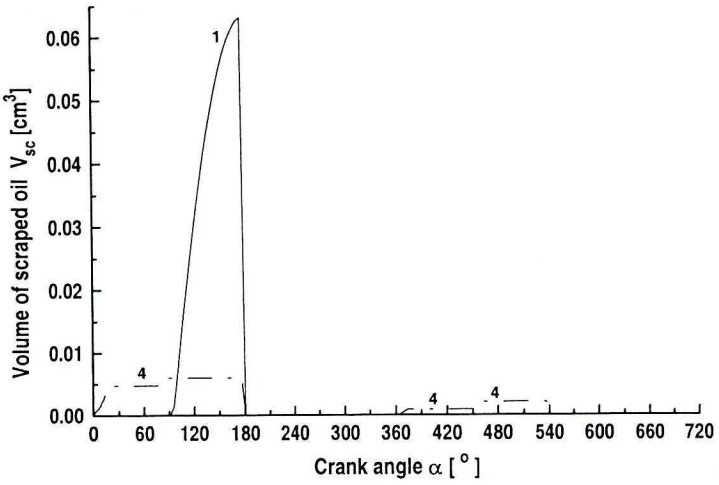

Fig. 17. Oil ejected to the combustion chamber (curve 1) or to crankcase (curve 4)

In Fig 17 it can be seen that the compression ring delivers oil to the combustion chamber during the compression phase of the engine cycle and that in the same phase the oil ring pumps oil from the gap between ring lip 3 and 4 (through the special channel) to the crankcase.

Depending on the oil film thickness, piston velocity and ring stiffness causes a variation in the ring land wetted area. Fully flooded ring lands in phases of low axial velocity are very often only partially flooded in areas of

high axial velocity. In Figs 18, 19 and 20 variations of the wetted area position are presented.

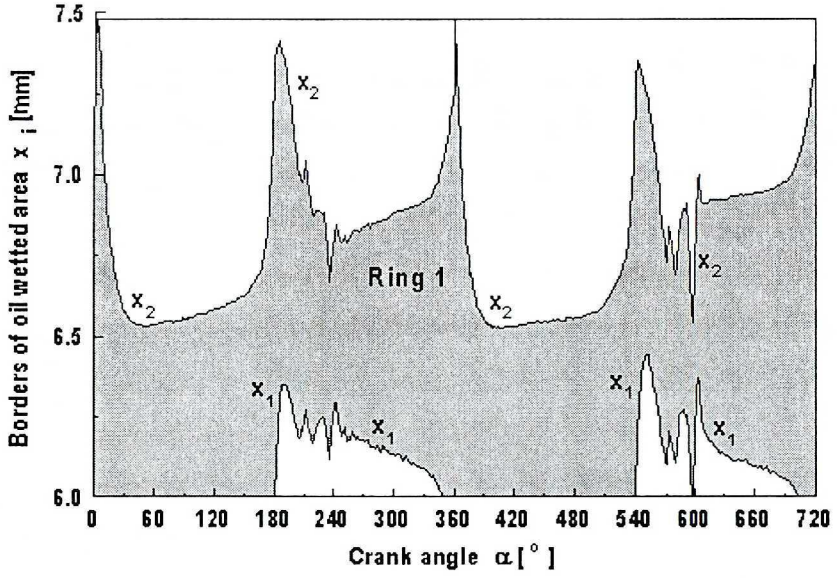

Fig. 18. Position of wetted area boundaries on the compression ring land as a function of crankshaft rotation, x_1 , x_2 – upper and lower boundaries

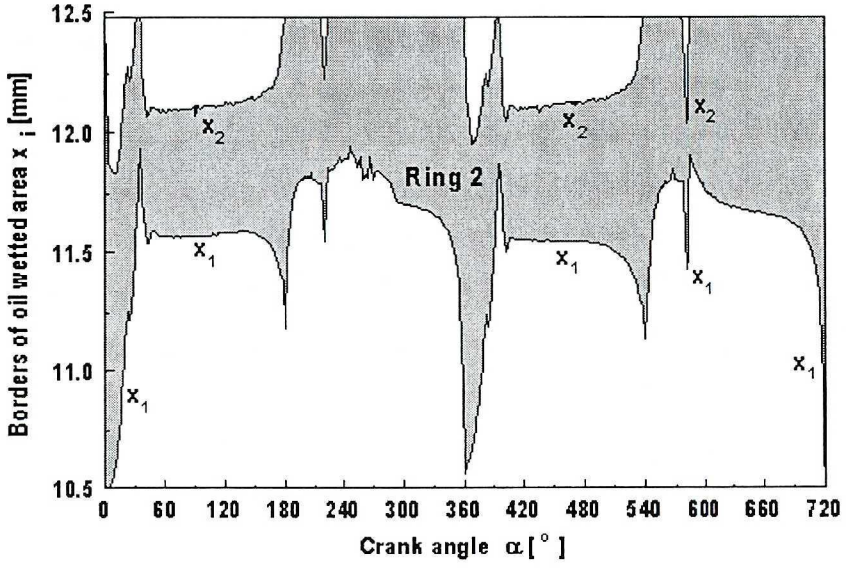

Fig. 19. Position of wetted area boundaries on scraper ring land as a function of crankshaft rotation x_1, x_2 – upper and lower boundaries

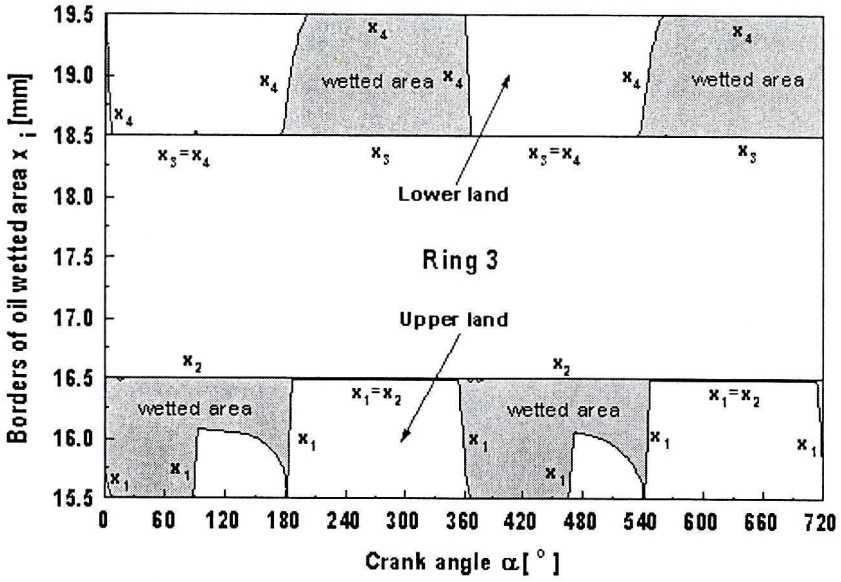

Fig. 20. Position of wetted area boundaries on oil ring lands as a function of crankshaft rotation x_1, x_2 – upper and lower boundaries of the upper land; x_3, x_4 – upper and lower boundaries of the lower land

Due to non-uniform oil film thickness on the liner, variable axial velocity and variable gas pressure acting on the ring, the wetted ring land area changes during the piston motion. In Fig 18, the position of the front and back wetted area boundaries on the upper ring (compression ring) are presented as functions of the crankshaft rotation. Sliding ring motion and ventilation of the divergent part of the gap between the liner and ring land (x_2 in phases 0–180 and 360–540 and x_1 in phases 180–360 and 540–720) can be seen in phases 180–360 and 540–720.

Fig. 19 presents the variation of wetted area boundaries for the second ring (scraper). Due to the different offset used in compression and scraper rings, the distribution of the wetted areas are also different. The ring scrapes oil towards the crankcase having only a small part of the ring land wetted.

The two-land oil ring shows a special pattern corresponding to the distribution of the wetted area. Depending on the direction of the piston motion, only the leading ring land is wetted while on the trailing land oil starvation can be observed.

9. Parametric study

The code described has been used for a parametric study of the influences of some parameter variation on the oil film distribution.

The height of the liner oil film strongly depends on the radius of the ring lip curvature. Rings having a smaller lip radius generate higher hydrodynamic force and form a thicker oil film. Generally, this is in conjunction with lower shear stress and lower friction losses.

New rings have a very high curvature radius of the ring lips. Due to the free motion of the ring in the piston groove the ring can tilt, and due to wear the shape of the ring lip changes, forming a lip with a smaller curvature radius. The level of freedom of the ring motion in the groove has a strong influence on the ring land curvature after a longer time period. The change in working conditions due to wear was simulated by the calculation of the ring pack operation for rings having different lip radius values.

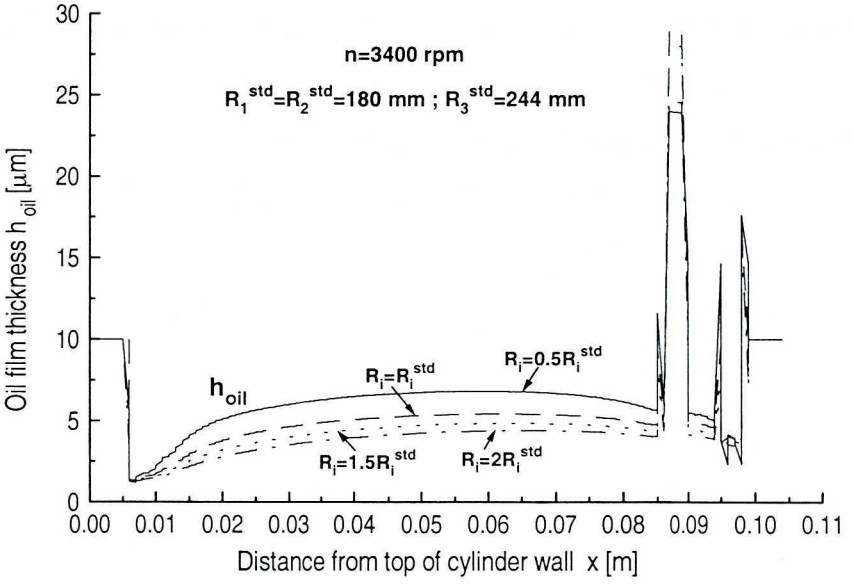

Fig. 21. Variation of the oil film distribution on the cylinder liner generated by ring packs with different ring land curvatures

In Fig. 21 one can see the influence of the ring land curvature on the thickness and distribution of the oil film on the cylinder liner. Rings having a lower radius of land curvature form thicker oil films.

Hydrodynamic forces generated in the gap between liner and ring lip are proportional to the ring axial velocity. During a cycle, the axial velocity tends to zero near the turning points. In these areas, the oil film thickness is strongly reduced, because the only force acting against the gas and ring stiffness forces is the hydrodynamic force generated by the squeeze velocity. This means that the squeeze velocity should be relatively high. Considering oil film thickness

distribution, differences depending on crankshaft rotational speed can be seen (Fig. 22).

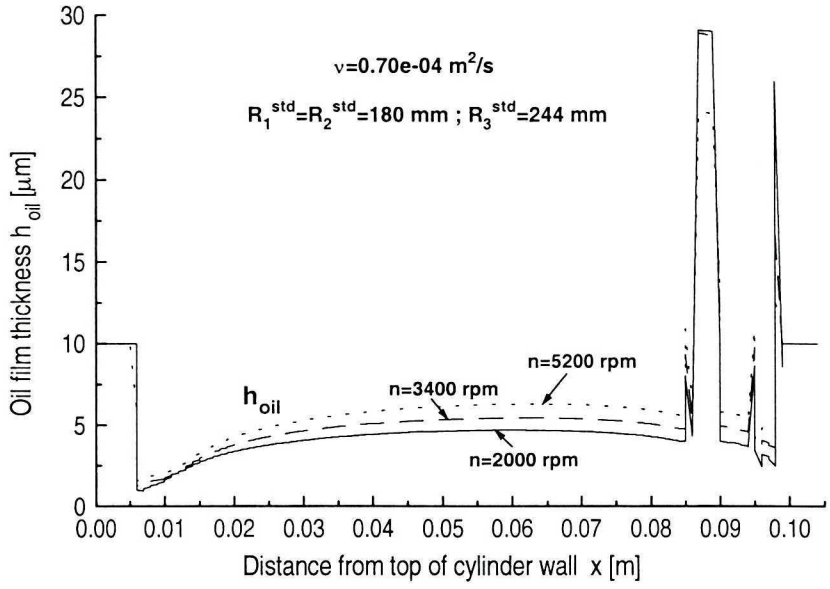

Fig. 22. Variation of the oil film distribution on the cylinder liner generated by the ring pack for different rotational velocities of the crankshaft

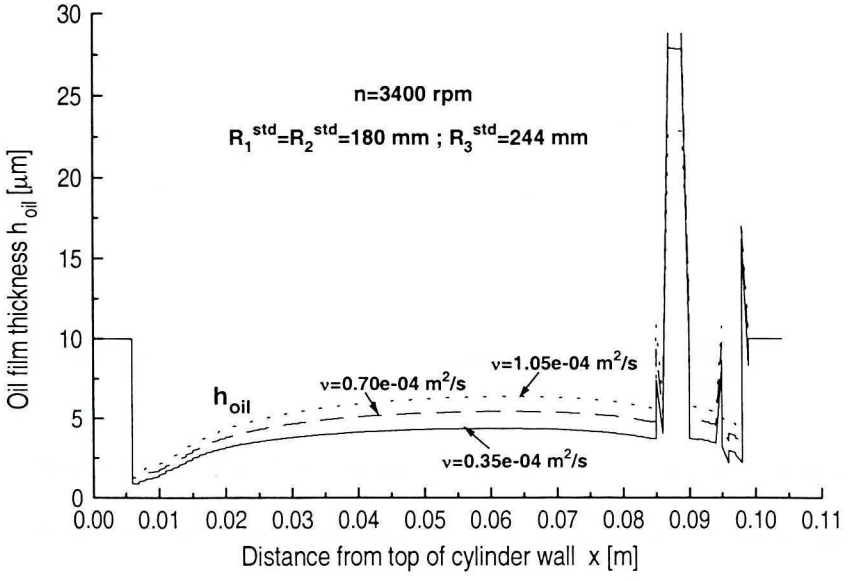

Fig. 23. Variation of the oil film distribution on the cylinder liner generated by a ring pack using oils of different viscosities

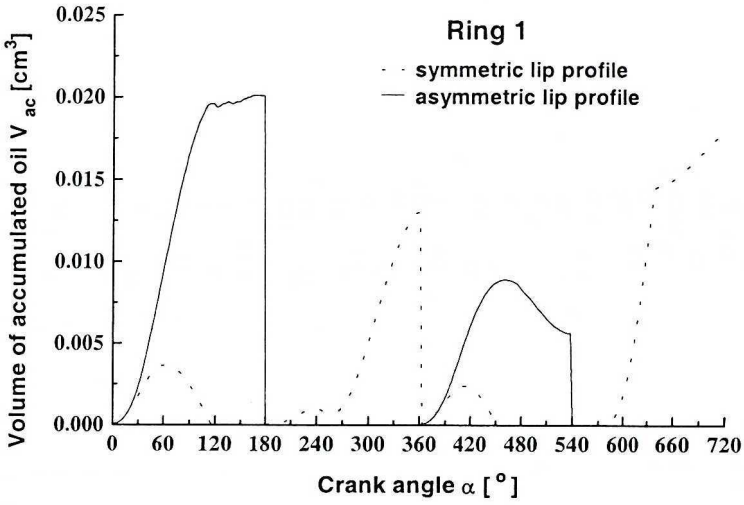

Fig. 24. Comparison of scraping efficiency of the symmetric and asymmetric ring lands (see also Fig. 6)

Oils of different types having generally different viscosities can be used for lubrication. Fig. 23 presents a comparison of the oil film thickness distribution for three values of the oil viscosity. The use of oils having lower viscosities results in a thinner oil film left by the ring pack on the cylinder liner.

Asymmetry of the ring land has a strong influence on the oil film thickness, oil transportation along the liner and oil redistribution (Fig. 24).

10. Conclusions

Equations, numerical method, and algorithm of solution and results of calculation of processes taking place in the gap between the ring land and cylinder surface in presence of the gas forces, have been presented in the paper. The influence of gas forces (acting on the backsides of the compression and scraper rings) on the oil film distribution and on the variation of wetted area boundaries for different types of ring (compression ring, scraper ring and oil ring) have been shown. The process of oil redistribution during the sliding motion of rings has been shown and analysed. The parametric calculation including the variation of ring land curvature radius, oil viscosity values, and piston velocity have been performed.

The computational code in the form presented can deliver a great deal of interesting information about the operation of the piston ring system, which would otherwise be unobtainable. Investigation of the influence of the ring

land shape on the formation of the oil film and oil transportation seems to be the one of fields of activity. The lack of reliable data concerning the ring land profile shape is the main problem in wider use of the code.

The possibilities of calculation of the mix-lubrication phenomenon will be included in the next version of the program.

The analysis of a mix-lubrication phenomena, the influence of temperature variation and shear stress on the oil viscosity and oil film thickness will be the subject of the second part of the paper.

Manuscript received by Editorial Board, August 28, 2003;
final version, October 17, 2003

REFERENCES

[1] Gulwadi S. D.: Analysis of Tribological Performance of a Piston Ring Pack. Tribology Transaction. Vol. 43, No. 2, pp. 151÷162, 2000.

[2] Iskra A.: Oelverbrauch eines Verbrennungsmotors. Tribologie/Schmierungstechnik 40, Heft 1, pp. 3÷9, 1993.

[3] Jeng Y.-R.: Theoretical Analysis of Piston-Ring Lubrication. Part I – Fully Flooded Lubrication. Part II – Starved Lubrication and Its Application to a Complete Ring Pack. Tribology Transactions. Vol. 35, No. 2, pp. 696÷705 and Vol. 4, pp. 707÷714, 1992.

[4] Keribar R., Dursunkaya Z., Flemming M. F.: An Integrated Model of Ring Pack Performance. ASME Transactions, Vol. 113, pp. 382÷389, 1991.

[5] Knopf M.: Bewertung der Zuverlässigkeit des tribologischen Systems Kolbenring-Zylinderlaufbüchse. Fortschr.-Ber., VDI Reihe 1, Nr. 266, VDI-Verlag, Düsseldorf, 1996.

[6] Kornprobst H., Woschni G., Zeilinger K.: Simulation des Kolbenring-Verhaltens im Motorbetrieb. Teil 1 und 2, Motortechnische Zeitschritt (MTZ) 50, Heft 11, pp. 528÷533 und Heft 12, pp. 582÷585, 1989.

[7] Kuo T.-W., Sellnau M. C., Theobald M. A., Jones J. D.: Calculation of Flow in the Piston-Cylinder-Ring Crevices of a Homogenous-Charge Engine and Comparison with Experiment, SAE Paper, No. 890838, 1989.

[8] Ma M.-T., Smith E. H., Sherrington I.: A Three-Dimensional Analysis of Piston Ring Lubrication. Part 1: Modelling. Proc. Inst. Mech. Eng., Vol. 209, 1995.

[9] Niewczas A.: Durability of a piston–piston rings–cylinder system of internal combustion engine (in Polish). WNT, Warsaw 1998.

[10] Radcliffe C.D., Dowson D.: Analysis of Friction in a Modern Automotive Piston Ring Pack, Lubricant and Lubrication. D. Dowson et al. (editors), Elsevier Science B.V., 1995.

[11] Ruddy B.L., Dowson D., Economous P.N.: A Theoretical Analysis of the Twin-Land Type of Oil-Control Piston Ring. Journal Mechanical Engineering Science, Vol. 23, No. 2, pp. 51÷62, 1981.

[12] Ruddy B.L., Dowson D., Economous P.N.: The Prediction of Gas Pressures within the Ring Packs of Large Bore Diesel Engines. Journal Mechanical Engineering Science, Vol. 23, No. 6, pp. 295÷304, 1981.

[13] Taylor C. M.: Engine Tribology. Elsevier Publishers B.V., 1993.

[14] Tian T., Wong V. W., Heywood B.: A Piston Ring Pack Film Thickness and Friction Model for Multigrade Oils and Rough Surfaces. SAE Paper, No. 962032, pp. 27÷39, 1996.

[15] Ting L. L.: Piston Ring Lubrication and Cylinder Bore Wear Analyses. Part II – Theory Verification. ASME Transactions, pp. 258÷266, April 1974.

Numeryczna symulacja pracy pakietu pierścieni tłokowych

Streszczenie

W pracy przedstawiono model ruchu zestawu pierścieni tłokowych przemieszczających się po filmie olejowym. W modelu uwzględniono siły hydrodynamiczne i siły sprężystości pierścieni, jak też siły gazowe działające na poszczególne pierścienie. Analizowano ruch pierścieni przy ich pełnym i częściowym zwilżeniu. Pokazano wpływ prędkości obrotowej silnika, profilu pierścieni, lepkości oleju na promieniowe ruchy poszczególnych pierścieni i grubość pozostałego filmu olejowego. Wyniki obliczeń przedstawiono w formie wykresów.